DAMTP-2015-72, IPPP/15/63, DCPT/15/124, TUM-HEP-1027-15

The ATLAS Di-boson Excess Could Be an $R-$parity Violating Di-smuon Excess

B. C. Allanach*
Department of Applied Mathematics and Theoretical Physics, Centre for Mathematical Sciences, University of Cambridge, Wilberforce Road, Cambridge CB3 0WA, UK

P. S. Bhupal Dev†
Physik Department T30d, Technische Universität München, James-Franck-Straße 1, D-85748 Garching, Germany

Kazuki Sakurai‡
Institute for Particle Physics Phenomenology, Ogden Centre for Fundamental Physics, Department of Physics, University of Durham, Science Laboratories, South Road, Durham DH1 3LE, UK

(Dated: January 22, 2016)

We propose a new possible explanation of the ATLAS di-boson excess: that it is due to heavy resonant slepton production, followed by decay into di-smuons. The smuon has a mass not too far from the W and Z masses, and so it is easily confused with W or Z bosons after its subsequent decay into di-jets, through a supersymmetry violating and $R-$parity violating interaction. Such a scenario is not currently excluded by other constraints and remains to be definitively tested in Run II of the LHC. Such light smuons can easily simultaneously explain the discrepancy between the measurement of the anomalous magnetic moment of the muon and the Standard Model prediction.

I. INTRODUCTION

In 20.3 fb^{-1} of $\sqrt{s} = 8$ TeV LHC data, ATLAS measured an excess with respect to Standard Model (SM) predictions in the production of di-electroweak gauge bosons VV (where $V = W, Z$) that decay hadronically [1]. The excess was at a di-boson invariant mass around 1.8–2 TeV, and occurred in all three decay channels: WZ, WW and ZZ with local significance of 3.4, 2.6 and 2.9σ, respectively.[1] The hadronically decaying di-bosons were identified by using jet mass and sub-jet grooming and mass-drop filtering techniques [3]. Despite some initial worries about the method of application of such techniques [4], they have so far held up to re-scrutinization theoretically [5]. ATLAS and CMS analyzed 3.2 and 2.2 fb^{-1} of Run II $\sqrt{s} = 13$ TeV data, respectively, and although no diboson excess above 2σ was found, the sensitivity was too small to rule out the Run I excess at the 95% confidence level (CL) [6, 7].

There have been many proposals of new physics in order to explain the Run I excess. Most of the early proposals involved the production of various different types of spin-one resonances [8–40]. There were also some attempts involving spin-zero [25, 28, 32, 41–48], spin-two [28, 42, 46] as well as composite fermion [49] resonances. However, none of these proposals involved sparticle resonances from the well-motivated minimal supersymmetric standard model (MSSM).[2] Here, we wish to construct a model that *is* consistent with the MSSM and that explains the ATLAS di-boson excess, thus potentially additionally solving the technical hierarchy problem and reinvigorating the hopes of confirming low-scale supersymmetry (SUSY) in Run II of the LHC. We take advantage of the fact that the ATLAS di-boson excess only relies on the mass of boosted jets in order to identify W and Z bosons. If the heavy resonance decays instead to other states which have a mass in the vicinity of the W and Z and then each of them decays to di-jets (which, because of the large resonance mass, look like one boosted fat jet with a two sub-jet structure), this scenario will not be distinguished from the VV resonance in the ATLAS analysis.

The rest of the paper is organised as follows: in Section II, we present the basic idea involving light smuons and test their compatibility with the existing constraints. A general discussion of the smuon masses and mixing is given in Section III, followed by the mass assignments in our RPV scenario in Section IV and the slepton decay widths in Section V. A fit to the di-boson excess is presented in Section VI. Some discussions followed by our conclusion are given in Section VII.

II. THE PROPOSAL

Our proposal is depicted in Fig. 1, where each vertex is $R-$parity violating (RPV). There are three independent vertices, requiring three different interaction terms in the RPV MSSM. We write the relevant part of the

* B.C.Allanach@damtp.cam.ac.uk
† bhupal.dev@tum.de
‡ kazuki.sakurai@durham.ac.uk

[1] It is interesting to note that a similar previous Run I search by CMS also had an excess, albeit milder, around the same mass [2].

[2] One attempt [50] did use a sgoldstino resonance: a spin-zero component of the goldstino. Such a scenario requires a fundamental supersymmetry breaking scale at a few TeV.

RPV superpotential (for a review, see e.g. [51])

$$W_{\rm LV} \;=\; \lambda'_{j11} L_j Q_1 \bar{D}_1 + \lambda'_{2kl} L_2 Q_k \bar{D}_l \;, \qquad (1)$$

along with a soft supersymmetry breaking and RPV term

$$\mathcal{L}_{\rm LV}^{\rm soft} \;=\; A_{j22} \tilde{\ell}_j \tilde{\ell}_2 \tilde{\mu}_R^+ + ({\rm H.c.}) \;, \qquad (2)$$

where $j,k,l \in \{1,\ 3\}$ are the family indices, Q_k and L_k are k^{th} generation quark and lepton doublet superfields respectively, and D_k is the k^{th} down-type quark singlet superfield. For the components of $\tilde{\ell}_j = (\tilde{\nu}_j, \tilde{\ell}_j^{\pm})$, there are two relevant λ'-type vertices from Eq. (1) which appear in Fig. 1, viz. $\lambda'_{j11}(\tilde{\nu}_j d_L \bar{d}_R - \tilde{\ell}_j^{\pm} u_L \bar{d}_R)$. Here we have only considered first-generation quarks in the initial states, as they have much larger parton distribution functions (PDFs) inside the proton than the other two generations. We could replace all of the family indices that are set to 2 in Eqs. (1) and (2) to a common but different value (as long as it were different to j), in which case we would really have di-stau or di-selectron production (throughout this paper, we implicitly include other modes involving the accompanying sneutrinos). For definiteness, and because it can potentially explain the long-standing discrepancy of the SM prediction with the measurement of the anomalous magnetic moment of the muon (see e.g. [52]), we focus here on the di-smuon case, but bear in mind that the other cases would lead to an identical signature at the LHC. The choice of k and l are irrelevant to the gross phenomenology, since any choice results in light sub-jets. The choice of j does affect whether one can obtain constraints and signals from neutrinoless beta decay ($0\nu\beta\beta$) [53, 54]. We shall comment on this possibility later. We ban baryon number violating terms from the RPV model (for example by using baryon triality [55]) in order to keep the proton stable, in accordance with observed lower limits on the proton decay lifetime [56]. Other lepton number violating terms may be present, but should be sub-dominant to the terms that we have written in Eqs. (1) and (2) in order for our analysis to be valid. We shall also set other sparticles not involved to be sufficiently heavy so that they do not interfere with our analysis or the di-boson signal.

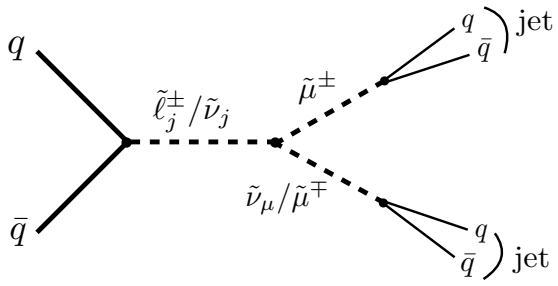

FIG. 1. Slepton resonance mimicking the ATLAS di-boson excess. The resonant charged slepton/sneutrino has a mass of around 1.9 TeV and the smuons must be in the mass regime 80-105 GeV, such that they would be mistaken for W or Z's after their boosted hadronic decay.

The ATLAS di-boson analysis [1] tagged a fat jet as a W if its mass was in the range $69.4 < m_j/{\rm GeV} < 95.4$ after grooming and filtering, whereas it was tagged as a Z if $79.8 < m_j/{\rm GeV} < 104.8$. There is clearly an overlap between the W and Z tags, and therefore, the WW, WZ and ZZ tagged regions are not completely disjoint (see Ref. [21] for a detailed statistical analysis including the overlaps). We must make sure that the smuons or muon sneutrinos in Fig. 1 are in the mass range $69.4 < m_{\tilde{\mu}}/{\rm GeV} < 104.8$ so that they are tagged as W and/or Z bosons. On the other hand, LEP II 4-jet searches [57] provide a lower bound on the smuon mass of around 77 GeV, as shown in Fig. 2, where we plot the 95% CL exclusion limits for the di-smuon production cross-section at $\sqrt{s} = 209$ GeV, as well as the corresponding model predictions, as a function of the smuon mass assuming the smuons predominantly decay into di-jets. The exclusion region depicted is on left-handed smuons and is more stringent than the one on right-handed smuons. The limit on muon sneutrinos is, to a very good approximation, identical to the limit on left-handed smuons. The corresponding cross section limits from $\sqrt{s} = 8$ TeV LHC (which are similar to the stop pair production limits) are even weaker; see e.g. [58]. From Fig. 2 we see that if we have smuons with mass larger than 80 GeV, then our scenario should not fall afoul of

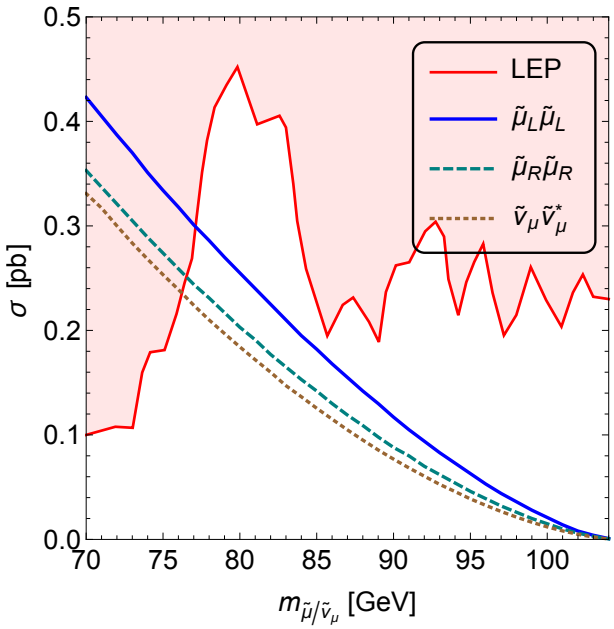

FIG. 2. 95% CL exclusion region (red shaded) derived from LEP II data for di-smuon production cross sections, followed by smuon decay into di-jets, as a function of the smuon mass. For comparison, we also show the pair production cross-sections for $\tilde{\mu}_L$ (blue solid), $\tilde{\mu}_R$ (green dashed) and $\tilde{\nu}_\mu$ (brown dotted) at $\sqrt{s} = 209$ GeV.

the LEP II limits. We shall therefore only use smuons in the range $80 < m_{\tilde{\mu}}/\text{GeV} < 105$.

This possibility is intriguing because the necessarily light smuons and muon sneutrinos will contribute to the anomalous magnetic moment of the muon $(g-2)_\mu$, measurements of which [59] have long been known to be discrepant with the SM at the 3.6σ level, with $\delta a_\mu \equiv \delta(g-2)_\mu/2 = (2.9 \pm 0.8) \times 10^{-9}$ [52]. However, SUSY gives one-loop contributions with smuons and neutralinos running in a loop, along with a loop containing muon sneutrinos and charginos, yielding [60]

$$\delta a_\mu \approx 1.3 \times 10^{-9} \left(\frac{100 \text{ GeV}}{\min(M_{\chi_1^\pm},\ M_{\chi_1^0})} \right)^2 \tan\beta \,\text{sign}(\mu M_2), \tag{3}$$

where the masses of smuons and muon sneutrinos are assumed to be around 100 GeV, $M_{\chi_1^\pm}$ and $M_{\chi_1^0}$ are the masses of the lightest chargino and the lightest neutralino, respectively, μ and M_2 are the Higgsino and wino mass parameters, respectively, and $\tan\beta \equiv v_u/v_d$ is the ratio of the up and down-type Higgs vacuum expectation values.[3] Given that $\tan\beta \lesssim 50$ from perturbativity and precision electroweak constraints [63], whereas $M_{\chi_1^\pm} \gtrsim 104$ GeV from LEP constraints [64], it appears that there is still plenty of viable parameter space where the discrepant $(g-2)_\mu$ measurement is explained by sparticle loops.

One may worry that such light smuons would be ruled out by di-jet constraints from the LHC [65–68], through $q'\bar{q} \to \tilde{\mu} \to q'\bar{q}$, but in fact the RPV coupling mediating such a process, λ'_{2kl}, may be made small enough ($\lesssim 10^{-2}$) to relax the di-jet constraint through suppression of the production cross-section, whereas the smuons in Fig. 1 will always still decay into $q\bar{q}$ as long as there are no other competing decay modes. LHC di-jet constraints from resonant smuon production [69] are proportional to $|\lambda'_{211}|^2$, which we may set to be arbitrarily small without affecting the di-boson signal. The smuon width is

$$\Gamma(\tilde{\mu} \to \bar{u}d) \;=\; \frac{3}{16\pi}|\lambda'_{211}|^2 m_{\tilde{\mu}}\,, \tag{4}$$

resulting in a decay length of

$$\text{L/cm} \;=\; 10^{-14}(\boldsymbol{\beta\gamma}) \left(\frac{100 \text{ GeV}}{m_{\tilde{\mu}}}\right) \frac{1}{3|\lambda'_{211}|^2}\,, \tag{5}$$

where $\boldsymbol{\beta}$ and $\boldsymbol{\gamma}$ are the usual relativistic kinematic factors. As long as $\lambda'_{211} > \mathcal{O}(10^{-6})$, the majority of the decays should occur promptly.

[3] Using `GM2Calc` [61], we have numerically verified that the linear dependence on $\tan\beta$ in Eq. (3) is an approximation good to around 20% for small to moderate $\tan\beta$ values, which will be the case for our benchmark point discussed later. For large $\tan\beta$, higher-order terms can become important and change this linear dependence [62].

Another potential problem is the fact that smuons and muon sneutrinos that are too light might be ruled out by precision electroweak constraints. Determining their contributions to the electroweak parameters S and T [70], Fig. 3 of Ref. [63] shows that even if *all three* left-handed slepton doublets have a mass of 100 GeV, at $\tan\beta = 2$, one obtains $\Delta S = -0.05$ and $\Delta T = 0.0$, well within the 90% CL bound. With only one slepton doublet required to be so light, we stay on the allowed side of the bound. In order to estimate whether the Tevatron may have ruled the scenario out, we estimated the total production cross-section for smuons and muon sneutrinos at $\sqrt{s} = 1.96$ TeV proton-anti-proton collisions with `Herwig7.0` [71, 72] to be 41 fb. Such a low cross-section for a 4-jet final state is not excluded by any Tevatron search, to the best of our knowledge.

III. THE SMUON MASSES AND MIXING

Without light right-handed neutrinos, the mass eigenstate coincides with the gauge eigen-state in the sneutrino sector. The mass of the muon sneutrino is given by

$$m^2_{\tilde{\nu}_\mu} \;=\; m^2_{\tilde{\ell}_2} + \frac{1}{2} m_Z^2 \cos 2\beta\,, \tag{6}$$

where $\tan\beta = v_u/v_d$ denotes the ratio of the vacuum expectation values of the two Higgs doublets H_u and H_d in the MSSM. In the gauge eigen-basis $(\tilde{\mu}_L, \tilde{\mu}_R)$, the smuon mass matrix is given by

$$M^2_{\tilde{\mu}} \;=\; \begin{pmatrix} \tilde{m}_L^2 & X_\mu \\ X_\mu & \tilde{m}_R^2 \end{pmatrix} \tag{7}$$

$$\begin{aligned} \text{with} \quad \tilde{m}_L^2 &= m^2_{\tilde{\ell}_2} + m_\mu^2 + m_Z^2 \cos 2\beta \left(-\frac{1}{2} + \sin^2\theta_w\right)\,, \\ \tilde{m}_R^2 &= m^2_{\tilde{\mu}_R} + m_\mu^2 - m_Z^2 \cos 2\beta \sin^2\theta_w\,, \\ X_\mu &= m_\mu(A_\mu - \mu\tan\beta)\,, \end{aligned} \tag{8}$$

θ_w being the weak mixing angle. This mass matrix is diagonalized in the mass eigen-basis $(\tilde{\mu}_1, \tilde{\mu}_2)$:

$$\begin{pmatrix} m^2_{\tilde{\mu}_2} & 0 \\ 0 & m^2_{\tilde{\mu}_1} \end{pmatrix} \;=\; U M^2_{\tilde{\mu}} U^\dagger, \qquad U = \begin{pmatrix} c_{\theta_\mu} & s_{\theta_\mu} \\ -s_{\theta_\mu} & c_{\theta_\mu} \end{pmatrix}, \tag{9}$$

where $c_{\theta_\mu} \equiv \cos\theta_\mu$, $s_{\theta_\mu} \equiv \sin\theta_\mu$ and

$$m^2_{\tilde{\mu}_{2,1}} = \frac{1}{2}\Big[(\tilde{m}_L^2 + \tilde{m}_R^2) \pm \sqrt{(\tilde{m}_L^2 - \tilde{m}_R^2)^2 + 4X_\mu^2}\Big], \tag{10}$$

$$\tan 2\theta_\mu = \frac{2X_\mu}{\tilde{m}_L^2 - \tilde{m}_R^2}\,. \tag{11}$$

The gauge and mass eigenbases are related by [cf. Eq. (9)] $\mu_L = c_{\theta_\mu}\widetilde{\mu}_2 - s_{\theta_\mu}\widetilde{\mu}_1$ and $\mu_R = s_{\theta_\mu}\widetilde{\mu}_2 + c_{\theta_\mu}\widetilde{\mu}_1$. Thus, one can find the Feynman rules for the vertices induced by Eq. (2) in the mass eigenbasis as

$$\tilde{\ell}_j^- \tilde{\nu}_\mu \tilde{\mu}_R^+ \;=\; \tilde{\ell}_j^- \tilde{\nu}_\mu (s_{\theta_\mu}\widetilde{\mu}_2^+ + c_{\theta_\mu}\widetilde{\mu}_1^+)\,, \tag{12}$$

$$\begin{aligned} \tilde{\nu}_j \tilde{\mu}_L^- \tilde{\mu}_R^+ \;=\; \tilde{\nu}_j (& c_{\theta_\mu} s_{\theta_\mu} \widetilde{\mu}_2^+ \widetilde{\mu}_2^- - c_{\theta_\mu} s_{\theta_\mu} \widetilde{\mu}_1^+ \widetilde{\mu}_1^- \\ & + c^2_{\theta_\mu} \widetilde{\mu}_1^+ \widetilde{\mu}_2^- - s^2_{\theta_\mu} \widetilde{\mu}_2^+ \widetilde{\mu}_1^-). \end{aligned} \tag{13}$$

Ignoring for now the di-jet decay mode via the $\lambda'_{j11}L_jQ_1\bar{D}_1$ operator, the ratio of the partial decay widths of the slepton resonance to di-smuons can be written as

$$\tilde{\ell}_j^{\pm} \;\to\; \tilde{\nu}_\mu\widetilde{\mu}_2^{\pm} : \tilde{\nu}_\mu\widetilde{\mu}_1^{\pm} \;=\; s^2_{\theta_\mu} : c^2_{\theta_\mu}\,, \tag{14}$$

$$\tilde{\nu}_j \;\to\; \widetilde{\mu}_2^{+}\widetilde{\mu}_2^{-} : \widetilde{\mu}_1^{+}\widetilde{\mu}_1^{-} : \widetilde{\mu}_2^{\pm}\widetilde{\mu}_1^{\mp} \;=\; \frac{s^2_{2\theta_\mu}}{4} : \frac{s^2_{2\theta_\mu}}{4} : 1 - \frac{s^2_{2\theta_\mu}}{2}\,, \tag{15}$$

independent of the A-parameter in Eq. (2). However, in practice, the λ'-terms in Eq. (1) also induce di-jet modes $\tilde{\ell}_j^{\pm} \to q\bar{q}'$ and $\tilde{\nu}_j \to q\bar{q}$, which cannot be neglected, since the same coupling is responsible for the production of the slepton resonance in Fig. 1, and hence, cannot be arbitrarily suppressed. Thus, the relative branching ratios of $\tilde{\ell}_j$ to di-smus will depend on both A_{j22} and λ_{j11}, as we will see in Section V.

IV. MASS ASSIGNMENT

In order to explain the di-boson excess by the $\tilde{\ell}_j$ production, two possibilities can be considered. One is to make $\tilde{\mu}_2$ heavy and explain the di-boson excess by identifying fat W/Z jets as fat $\widetilde{\mu}_1/\tilde{\nu}_\mu$ jets. If one requires the $\tilde{\ell}_j^{\pm}$ production contributes to the di-boson excess, $m_{\tilde{\nu}_\mu} \simeq \tilde{m}_L$ has to be around the gauge boson mass, $m_V \simeq (m_Z + m_W)/2$. To remove the $\tilde{\mu}_2$ contribution from the signal, we need $\tilde{m}_R \gg m_V$. Assuming $X_\mu \ll \tilde{m}_R$, the lighter smuon mass can be written as [cf. Eq. (10)]

$$m^2_{\widetilde{\mu}_1} \;\simeq\; \tilde{m}_L^2 - \frac{2X_\mu^2}{\tilde{m}_R^2 - \tilde{m}_L^2}\,. \tag{16}$$

Therefore, to make $m^2_{\widetilde{\mu}_1}$ positive and also around the gauge boson mass, $X_\mu \ll \tilde{m}_R$ is indeed necessary. From Eq. (11) and knowing $\widetilde{\mu}_1 \sim \tilde{\mu}_L$, one can see that $\theta_\mu \sim \frac{\pi}{2}$ and the couplings for the $\tilde{\ell}_j^{\pm} \to \tilde{\nu}_\mu\widetilde{\mu}_1^{\pm}$ and $\tilde{\nu}_j \to \widetilde{\mu}_1^{+}\widetilde{\mu}_1^{-}$ are suppressed by $\cos^2\theta_\mu$ and $\sin^2 2\theta_\mu/4$, respectively. Thus in this case, the di-jet final state can more easily dominate the $\tilde{\ell}_j$ decay, instead of the di-smuon final state, disfavoring our RPV interpretation.

Another possibility is to bring down the masses of all particles in the smuon sector, i.e. $\tilde{\nu}_\mu, \widetilde{\mu}_1$ and $\widetilde{\mu}_2$, to around the average gauge boson mass scale m_V. If one demands $(m_{\widetilde{\mu}_2}, m_{\widetilde{\mu}_1}) \simeq (m_Z, m_W)$, both $\tilde{m}_L^2$ and $\tilde{m}_R^2$ have to be around the gauge boson mass scale, and $(\tilde{m}_L^2 - \tilde{m}_R^2)$, X_μ have to be smaller than m_V, being related by

$$(m_Z^2 - m_W^2)^2 \simeq (\tilde{m}_L^2 - \tilde{m}_R^2)^2 + 4X_\mu^2\,. \tag{17}$$

One can also find

$$s_{2\theta_\mu} \;\simeq\; \frac{A_\mu - \mu\tan\beta}{8651\,\mathrm{GeV}}\,, \quad c_{2\theta_\mu} \;\simeq\; \frac{\tilde{m}_L^2 - \tilde{m}_R^2}{1881\,\mathrm{GeV}^2}\,. \tag{18}$$

In this case, all decay modes in Eqs. (14) and (15) are possible and the mixing can be suppressed as long as the smuon decays are prompt because the $\tilde{\mu}_{1,2} \to q\bar{q}$ decay widths are proportional to $|\lambda'_{211}s_{\theta_\mu}|^2$ and $|\lambda'_{211}c_{\theta_\mu}|^2$, respectively.

For example, by taking $\tan\beta = 1.5$, $m_{\tilde{\ell}_2} = 88\,\mathrm{GeV}$, $m_{\tilde{\mu}_R} = 80\,\mathrm{GeV}$, $X_\mu = 537\,\mathrm{GeV}^2$, we find

$$\begin{aligned}
m_{\tilde{\nu}_\mu} &= 78.43\,\mathrm{GeV}\,,\\
m_{\widetilde{\mu}_1} &= 83.43\,\mathrm{GeV}\,,\\
m_{\widetilde{\mu}_2} &= 93.68\,\mathrm{GeV}\,,\\
\sin\theta_\mu &= 0.31\,,\\
\tilde{\ell}_j^{\pm} \to \tilde{\nu}_\mu\widetilde{\mu}_2^{\pm} : \tilde{\nu}_\mu\widetilde{\mu}_1^{\pm} &= 0.097 : 0.903\,,\\
\tilde{\nu}_j \to \widetilde{\mu}_2^{+}\widetilde{\mu}_2^{-} : \widetilde{\mu}_1^{+}\widetilde{\mu}_1^{-} : \widetilde{\mu}_2^{\pm}\widetilde{\mu}_1^{\mp} &= 0.0874 : 0.0874 : 0.8252\,,
\end{aligned} \tag{19}$$

We approximate $m_{\widetilde{\mu}_1}$ and $m_{\tilde{\nu}_j}$ by M_W and $m_{\widetilde{\mu}_2}$ by M_Z, since the values are rather close. Eq. (19) implies that $\tilde{\ell}_j^{\pm}$ mostly decays to $\tilde{\nu}_\mu\widetilde{\mu}_1^{\pm}$ and $\tilde{\nu}_j$ mostly to $\widetilde{\mu}_2^{\pm}\widetilde{\mu}_1^{\mp}$, thereby mimicking the WW and WZ final states, respectively, in the context of the ATLAS di-boson search. We note here that by playing with the mass parameters, we could change the effective proportions of WW, WZ or indeed ZZ final states. We shall here stick to the approximation that $\tilde{\ell}_j^{\pm}$ always decays to $\tilde{\nu}_\mu\widetilde{\mu}_1^{\pm}$ and $\tilde{\nu}_j$ always decays to $\widetilde{\mu}_2^{\pm}\widetilde{\mu}_1^{\mp}$.

V. SLEPTON DECAYS

In order to explain the di-boson excess through the resonant slepton production process of Fig. 1, we assume $M = m_{\tilde{\ell}_j^{\pm}} \simeq m_{\tilde{\nu}_j} \simeq 1.9\,\mathrm{TeV}$.[4] According to data, the resonance should not be too much wider than 100 GeV [1] (although perhaps up to 160 GeV or so is still acceptable). The decay width of $\tilde{\ell}_j^{\pm}/\tilde{\nu}_j$ to the smuon and muon sneutrinos induced by A_{2jj} from Eq. (2) is given by

$$\begin{aligned}
\Gamma(\tilde{\nu}_j \to \widetilde{\mu}_2^{+}\widetilde{\mu}_2^{-}, \widetilde{\mu}_1^{+}\widetilde{\mu}_1^{-}, \widetilde{\mu}_2^{\pm}\widetilde{\mu}_1^{\mp}) \;&\simeq\; \Gamma(\tilde{\ell}_j^{\pm} \to \tilde{\nu}_\mu\widetilde{\mu}_2^{\pm}, \tilde{\nu}_\mu\widetilde{\mu}_1^{\pm})\\
&=\; \frac{|A_{j22}|^2}{16\pi M}\left(1 - \frac{4m_{\tilde{\mu}}^2}{M^2}\right)^{1/2}\,.
\end{aligned} \tag{20}$$

On the other hand, the decay width for the $q\bar{q}$ mode through the λ'-term in Eq. (1) is given by

$$\Gamma(\tilde{\nu}_j \to q\bar{q}) \;\simeq\; \Gamma(\tilde{\ell}_j^{\pm} \to q\bar{q}) \;=\; \frac{3|\lambda'_{j11}|^2 M}{16\pi}. \tag{21}$$

The branching ratio for the $\tilde{\nu}_j$ to decay to smuons is therefore given by

$$\mathrm{BR}_{\tilde{\mu}} \;\simeq\; \frac{|A_{j22}|^2}{3|\lambda'_{j11}|^2M^2 + |A_{j22}|^2}\,. \tag{22}$$

[4] 1.9 TeV provides a good fit to the ATLAS di-boson excess and other CMS data [17, 73], although we could also have chosen 2 TeV, without affecting our main conclusions.

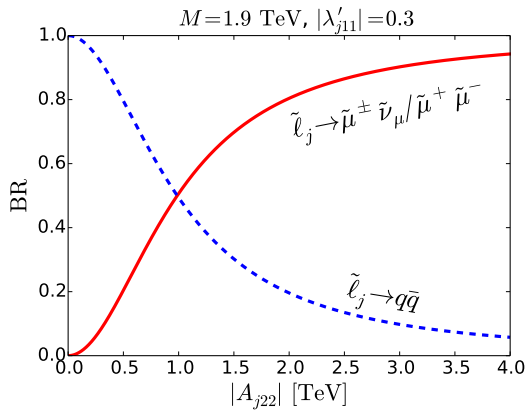

FIG. 3. Branching ratios of slepton decays to di-quark and di-smuon through RPV couplings given by Eqs. (1) and (2), respectively.

Here we have neglected the $\mathcal{O}(m^2_{\tilde{\mu}}/M^2)$ terms, keeping in mind the benchmark scenario given by Eq. (19). Fig. 3 shows the branching ratios for the smuon and di-jet final states as functions of $|A_{j22}|$, where $M = 1.9\,\text{TeV}$ and $|\lambda'_{j11}| = 0.3$ are assumed. It is clear that for large $|A_{j22}|$, the di-smuon decay mode will dominate over the di-jet mode, which is favorable for the di-boson excess. We note here that in principle, a very large A_{j22}-term could make the soft-mass squared $(m^2_{\tilde{\ell}})_{22}$ negative when running to higher renormalization scales, since the renormalization group (RG) evolution of the slepton mass Lagrangian term $(m^2_{\tilde{\ell}})_{22}$ has a piece $d(m^2_{\tilde{\ell}})_{22}/d\ln\mu = -2|A_{j22}|^2/(16\pi^2) + \ldots$ [74]. It is not clear immediately whether this would destabilize the electroweak vacuum, since loop corrections to the energy density of the minimum could be the same size as the tree-level potential [75]. In order to calculate any such constraint reliably, one can use the "RG-improved" potential, taking the renormalization scale to be the putative vacuum expectation value [76], which should in this case be around the TeV scale (because it is driven by the TeV scale parameter A_{j22}). Since this scale is not very far from the electroweak scale, there one does not have to run the RG equations very far and the constraints are likely to be weak because there is not much room for a tachyonic smuon to arise. There are other potential directions in scalar field space to check that are *not* associated with tachyons, but to reliably calculate bounds from those, one would have to upgrade a package like `Vevacious` [77] in order to include RPV, which is beyond the scope of this paper and might be studied elsewhere.

We must also consider whether the model is non-perturbative, since, for example, a loop correction to the quartic $\tilde{l}_j$ coupling may be large: the dominant diagram is a box with smuons/muon sneutrinos running in the loop. We find a one-loop correction to the coefficient of the effective potential term $V \supset \lambda_{\tilde{l}_j}|\tilde{l}_j|^4$, where $\lambda_{\tilde{l}_j} = (g_2^2 + g_1^2)/4$ at the tree-level (g_2 and g_1 being the $SU(2)_L$ and $U(1)_Y$ gauge couplings, respectively) [78, 79]

$$\Delta\lambda_{\tilde{l}_j} \approx -\frac{1}{384\pi^2}\left(\frac{A_{j22}}{\tilde{m}}\right)^4 , \tag{23}$$

assuming a common mass $\tilde{m}$ for the left-handed smuons and muon sneutrinos. Below, we shall impose that this correction is not too large, i.e.

$$|\lambda_{\tilde{l}_j} + \Delta\lambda_{\tilde{l}_j}| \;<\; 4\pi \; ; \tag{24}$$

otherwise, the theory would be non-perturbative and we would not be able to trust the accuracy of our results.

One might also worry whether the negative sign in Eq. (23) leads to a charge-breaking minimum (CBM) in the direction of the slepton [80, 81]. For a robust determination of whether this is unsafe for us, we need to compute the lifetime of this minimum. Here we will simply use a conservative constraint by demanding that the coefficient of the quartic-term in the one-loop effective potential is positive-definite, i.e.

$$\lambda_{\tilde{l}_j} + \Delta\lambda_{\tilde{l}_j} \;\geq\; 0 \, . \tag{25}$$

In any case, our RPV scenario with a light smuon is consistent with all current experimental constraints [51] and may be tested soon in the ongoing Run II phase of the LHC. For a detailed discussion of light smuon phenomenology at the LHC, see e.g. Refs. [74, 82].

VI. FITTING THE DI-BOSON EXCESS

We first calculate the resonant production cross sections for a 1.9 TeV $\tilde{\ell}_j^\pm$ or $\tilde{\nu}_j$ at $\sqrt{s} = 8$ TeV LHC using the RPV model implementation in `FeynRules` [83] and the parton-level event generation in `MadGraph5` [84] with `NNPDF2.3` leading order PDF sets [85]. We get

$$\sigma(pp \to \tilde{\ell}_j^\pm) \;=\; 75 \text{ fb} \, , \quad \sigma(pp \to \tilde{\nu}_j, \tilde{\nu}_j^*) \;=\; 359 \text{ fb} \, ,$$

normalized to $|\lambda'_{j11}|^2 = 1$. The decay width of $\tilde{\ell}_j \to \tilde{\nu}_\mu^\pm \tilde{\mu}$, $\tilde{\mu}^+\tilde{\mu}^-$ is given by Eq. (20) and that of $\tilde{l}_j \to q\bar{q}$ is given by Eq. (21). These are assumed to be the dominant decay modes so that the branching ratio to di-smuon is given by Eq. (22). The smuons (and muon sneutrinos) are assumed to decay into di-jets with a 100% branching ratio, as argued below Eq. (4), which is reasonable given that these are the lightest sparticles in the model. Ref. [21] unfolded cross-contamination of the WW, WZ and ZZ channels and estimates of the efficiencies to bound the case where one has contributions from all three channels. Here, after the approximations listed under Eq. (19), we have contributions to the WW-like channel from charged slepton production and from the WZ-like channel from sneutrino production, whereas we neglect any ZZ-like channel production. By referring to

the right-hand panel of Fig. 4 of Ref. [21], we see that the ATLAS constraint on the sum of $WW + WZ$ channels production cross section times branching ratio should be approximately $5 - 25$ fb to 95% CL. Our prediction for this quantity is

$$\sigma_{\rm sig.} \;=\; |\lambda'_{j11}|^2\, {\rm BR}_{\tilde\mu}\big[\sigma(pp\to\tilde\ell_j^\pm) + \sigma(pp\to\tilde\nu_j)\big]. \quad (26)$$

This favored region ('ATLAS8 diboson fav.') is shown by the blue shaded region in Figure 4. The corresponding CMS search for boosted di-bosons [2] has given a stringent 95% CL upper limit of 14.3 fb on the signal cross section for 1.9 TeV invariant mass, which excludes the green shaded region in Figure 4. Note that this is still consistent with a large part of the parameter space favoring the ATLAS di-boson excess. Furthermore, there is another stringent constraint coming from the LHC di-jet searches performed in Run-I [65, 66], and more recently, in early Run-II [67, 68], which are also applicable to $pp\to\tilde\ell_j^\pm/\tilde\nu_j\to q\bar q$. At $\sqrt{s}=8$ (13) TeV LHC, the cross section for a 1.9 TeV $q\bar q$ resonance must be smaller than 100 (400) fb [66, 67], which excludes at 95% CL the solid (dashed) orange shaded region in Figure 4. There are also theoretical constraints from perturbativity [cf. Eq. (24)] and CBM [cf. Eq. (25)], which are shown in Figure 4 by the horizontal red solid and pink dashed lines, respectively. We have not shaded the CBM region, since the CBM bound shown here should not be considered as a strict upper limit, unless and until one does a lifetime calculation, which is beyond the scope of this paper. In any case, we find that there still survives a resonable portion of the parameter space in our RPV scenario consistent with the ATLAS di-boson excess.

We note here that for the $j = 1$ case the λ'_{111} coupling also induces neutrinoless double beta decay ($0\nu\beta\beta$) [53, 54], and hence, constrained by the current experimental limits on $0\nu\beta\beta$ half-life. Using the latest 90% CL combined limit for ^{76}Ge isotope from GERDA phase-I [86], we find [87, 88]

$$|\lambda'_{111}| \;\lesssim\; 4.5\times10^{-4}\left(\frac{m_{\tilde e_L}}{100\ {\rm GeV}}\right)^2\left(\frac{m_{\tilde\chi_1^0}}{100\ {\rm GeV}}\right)^{1/2}. \quad (27)$$

For a selectron mass of 1.9 TeV as required here to explain the ATLAS di-boson excess, we obtain a mild upper limit of $|\lambda'_{111}|\lesssim 0.51$ for the lightest neutralino mass $m_{\tilde\chi_1^0}=1$ TeV, as shown by the dashed vertical line in Figure 4. From Eq. (27) and Fig. 4, we can readily infer that the $0\nu\beta\beta$ constraint still allows some parameter space favoring the ATLAS di-boson excess as long as the lightest neutralino is heavier than 150 GeV in our RPV scenario. If we were to re-fit for a slepton mass of 2 TeV, this line would be less restrictive and move to the right. The CMS dijet bound would moves slightly toward the left and there are other small changes, but the qualitative picture as shown in the Figure remains.

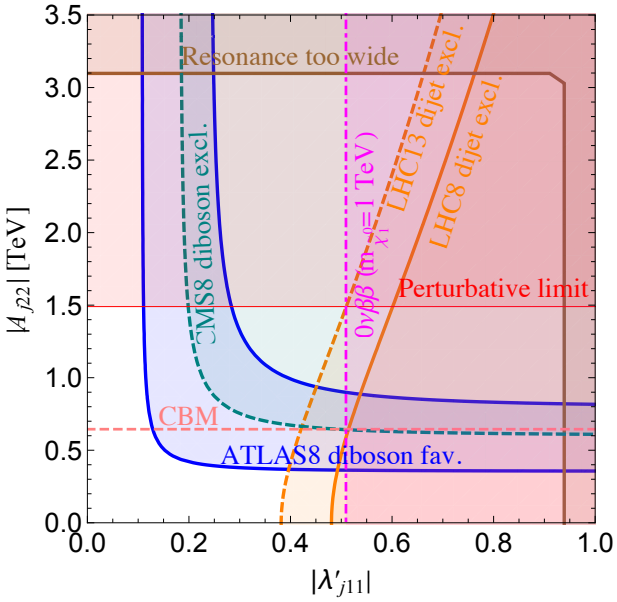

FIG. 4. The RPV parameter space favored by the ATLAS di-boson excess in 8 TeV LHC data (blue shaded region). The 8 TeV exclusion regions from CMS di-jet (solid orange) and di-boson (green), as well as the 13 TeV exclusion from CMS di-jet (dashed orange) searches are also shown. The magenta dashed vertical line shows the upper limit for the $j = 1$ case on $|\lambda'_{111}|$ due to null results from a recent $0\nu\beta\beta$ search, assuming the lightest neutralino mass of 1 TeV. The light red region in the top half of the plot is non-perturbative as estimated by Eq. (24) and the region outside of the solid brown line has a resonance width larger than 100 GeV. The horizontal pink dashed line is the suggestive upper bound for $|A_{j22}|$ obtained from Eq. (25) beyond which one might develop a charge-breaking minimum.

VII. DISCUSSION AND CONCLUSION

Before concluding, we wish to make a few comments on the testability of our scenario and its applicability to other potentially relevant excesses with respect to the SM predictions:

(i) The di-boson interpretation of the ATLAS excess inevitably leads to leptonic and semi-leptonic final states, along with the hadronic decays of the di-boson system. In contrast, our model, as currently written, does not predict leptonic decays of the smuons, thus providing a potential explanation of the absence of a corresponding di-boson excess in the leptonic or semi-leptonic channels [89, 90]. With more statistics pouring in from the Run II phase of the LHC, this will be a clear distinguishing feature of our scenario in the near future.

(ii) Unlike the W' interpretation of the ATLAS di-boson excess which involves WZ final states (see e.g. [9, 12, 17, 21, 34]), and hence, necessarily leads to

a WH excess (H being the SM Higgs boson) by virtue of the Goldstone equivalence theorem, our ATLAS di-boson favored region in Fig. 4 does not suffer from any such constraints. On the other hand, a recent CMS search [91] seems to suggest a mild global excess of 1.9σ in the WH channel with $H \to b\bar{b}$ and $W \to \ell\nu$.[5] If this excess becomes statistically significant, one way of accommodating it in our model is to have $m_{\tilde{\nu}_\mu} \simeq m_H$ and assume $\tilde{\nu}_\mu$ predominantly decays to $b\bar{b}$ through the λ'_{233} coupling. The leptonic W decay can also be mimicked by augmenting Eq. (1) with another RPV term $\lambda_{2kl} L_2 L_k \bar{E}_l$, where $k, l \in \{1,\ 3\}$, which will induce a non-zero branching ratio of $\tilde{\mu}^\pm \to \ell_l^\pm \nu_k$. Unlike W decays, we do not generically expect the leptonic decays of smuons to be flavor universal. Therefore, this could serve as another distinguishing feature of our scenario. Yet another difference with respect to the WZ final state is that it leads to a mono-jet signature in the decay channel $Z \to \nu\bar{\nu}$ and $W \to$a fat jet [94], whereas our scenario does not predict any such signatures.

(iii) In the case where we choose the indices labeled as '2' in Eqs. (1) and (2) to instead be '3', we have di-stau (or tau sneutrino) production. In this case, the analysis of the collider phenomenology proceeds similarly to the smuon case: the LEP constraints are identical. However, in the case of di-stau production, one does not address the discrepancy between the measurement and the SM prediction of $(g-2)_\mu$.

Interestingly, our scenario might explain some other Run I excesses, as follows: CMS searches for a right-handed charged gauge boson reported a 2.8σ excess in the $eejj$ final state [95]. In addition, the CMS search for di-leptoquark production has found a 2.4σ excess in the $eejj$ channel and a 2.6σ excess in the $e\nu jj$ channel [96]. It is possible to explain both of these excesses with resonant slepton production in RPV SUSY, which decays to a lepton and a chargino/neutralino, followed by three-body decays of the neutralino/chargino via an RPV coupling [97, 98]. In principle, it is also possible to simulataneously accommodate the ATLAS di-boson excess in this scenario, e.g. $pp \to \tilde{\ell}_1^\pm \to e\tilde{\chi}_1^0 \to ee\tau\tilde{\tau} \to eejj + p_T^{\rm miss}$. However, there are three potential problems with this solution: (a) the leptonic decay of the tau also gives muons, so we would expect $e\mu jj$ final states as well, which does not show any significant excess at the LHC so far; (b) the di-jets from a light smuon decay tend to be highly boosted, as discussed above; so the signal efficiency will drop drastically if we require well-separated jets to explain the CMS excesses; (c) the CMS excess in $eejj$ favors more opposite-sign di-electron final states, whereas the Majorana neutralino decays produces same-sign electrons with the same rate as opposite sign. A detailed analysis addressing these issues is beyond the scope of the current paper and is left for a future study.

In conclusion, we have presented a new supersymmetric interpretation of the ATLAS di-boson excess within an R-parity violating low-scale SUSY framework that *ab initio* does not predict leptonic branchings, although the model can be tweaked to predict them. In fact, a recent combination by ATLAS of its channels [99] shows that, once the leptonic channels are added, the global significance of the di-boson excess (assuming that the events consist of real WW, ZZ or WZ) goes down, indicating a better fit with only hadronic decays. In particular, we propose a sparticle spectrum with smuon masses in the 80-105 GeV range and a resonant 2 TeV slepton that can be tested in the Run II phase of the LHC. These necessarily light smuons are then in turn linked to the discrepancy between the measurement and SM prediction of the anomalous magnetic moment of the muon. If the di-boson excess persists and becomes statistically significant, it could potentially be the first sign of SUSY at the LHC.

VIII. ACKNOWLEDGMENTS

This work of B.C.A. has been partially supported by STFC grant ST/L000385/1. The work of P.S.B.D. is supported in part by a TUM University Foundation Fellowship and the DFG cluster of excellence "Origin and Structure of the Universe". B.C.A. and K.S. would like to thank TUM for hospitality extended during the conception of this work. We thank Ben O'Leary for helpful discussions regarding electroweak stability.

[1] G. Aad et al. (ATLAS) (2015), 1506.00962.
[2] V. Khachatryan et al. (CMS), JHEP **08**, 173 (2014), 1405.1994.
[3] J. M. Butterworth, A. R. Davison, M. Rubin, and G. P. Salam, Phys. Rev. Lett. **100**, 242001 (2008), 0802.2470.
[4] D. Gonalves, F. Krauss, and M. Spannowsky, Phys. Rev. **D92**, 053010 (2015), 1508.04162.
[5] G. Aad et al. (ATLAS) (2015), 1510.05821.
[6] Tech. Rep. ATLAS-CONF-2015-073, CERN, Geneva (2015), URL `http://cds.cern.ch/record/2114845`.
[7] Tech. Rep. CMS-PAS-EXO-15-002, CERN, Geneva (2015).
[8] H. S. Fukano, M. Kurachi, S. Matsuzaki, K. Terashi, and K. Yamawaki, Phys. Lett. **B750**, 259 (2015), 1506.03751.
[9] J. Hisano, N. Nagata, and Y. Omura, Phys. Rev. **D92**, 055001 (2015), 1506.03931.

[5] The corresponding ATLAS search [92] and a similar CMS search in the all-hadronic final states [93] have not reported any such excess though.

[10] D. B. Franzosi, M. T. Frandsen, and F. Sannino (2015), 1506.04392.
[11] K. Cheung, W.-Y. Keung, P.-Y. Tseng, and T.-C. Yuan (2015), 1506.06064.
[12] B. A. Dobrescu and Z. Liu (2015), 1506.06736.
[13] J. Aguilar-Saavedra (2015), 1506.06739.
[14] A. Alves, A. Berlin, S. Profumo, and F. S. Queiroz (2015), 1506.06767.
[15] Y. Gao, T. Ghosh, K. Sinha, and J.-H. Yu (2015), 1506.07511.
[16] A. Thamm, R. Torre, and A. Wulzer (2015), 1506.08688.
[17] J. Brehmer, J. Hewett, J. Kopp, T. Rizzo, and J. Tattersall, JHEP **10**, 182 (2015), 1507.00013.
[18] Q.-H. Cao, B. Yan, and D.-M. Zhang (2015), 1507.00268.
[19] G. Cacciapaglia and M. T. Frandsen, Phys. Rev. **D92**, 055035 (2015), 1507.00900.
[20] T. Abe, R. Nagai, S. Okawa, and M. Tanabashi, Phys. Rev. **D92**, 055016 (2015), 1507.01185.
[21] B. C. Allanach, B. Gripaios, and D. Sutherland, Phys. Rev. **D92**, 055003 (2015), 1507.01638.
[22] T. Abe, T. Kitahara, and M. M. Nojiri (2015), 1507.01681.
[23] A. Carmona, A. Delgado, M. Quirs, and J. Santiago, JHEP **09**, 186 (2015), 1507.01914.
[24] B. A. Dobrescu and Z. Liu, JHEP **10**, 118 (2015), 1507.01923.
[25] C.-W. Chiang, H. Fukuda, K. Harigaya, M. Ibe, and T. T. Yanagida (2015), 1507.02483.
[26] L. A. Anchordoqui, I. Antoniadis, H. Goldberg, X. Huang, D. Lust, and T. R. Taylor, Phys. Lett. **B749**, 484 (2015), 1507.05299.
[27] L. Bian, D. Liu, and J. Shu (2015), 1507.06018.
[28] D. Kim, K. Kong, H. M. Lee, and S. C. Park (2015), 1507.06312.
[29] K. Lane and L. Prichett (2015), 1507.07102.
[30] A. E. Faraggi and M. Guzzi (2015), 1507.07406.
[31] M. Low, A. Tesi, and L.-T. Wang, Phys. Rev. **D92**, 085019 (2015), 1507.07557.
[32] P. Arnan, D. Espriu, and F. Mescia (2015), 1508.00174.
[33] C. Niehoff, P. Stangl, and D. M. Straub (2015), 1508.00569.
[34] P. S. B. Dev and R. N. Mohapatra, Phys. Rev. Lett. **115**, 181803 (2015), 1508.02277.
[35] F. F. Deppisch, L. Graf, S. Kulkarni, S. Patra, W. Rodejohann, N. Sahu, and U. Sarkar (2015), 1508.05940.
[36] L. Bian, D. Liu, J. Shu, and Y. Zhang (2015), 1509.02787.
[37] R. L. Awasthi, P. S. B. Dev, and M. Mitra (2015), 1509.05387.
[38] T. Li, J. A. Maxin, V. E. Mayes, and D. V. Nanopoulos (2015), 1509.06821.
[39] J. H. Collins and W. H. Ng (2015), 1510.08083.
[40] H. S. Fukano, S. Matsuzaki, K. Terashi, and K. Yamawaki (2015), 1510.08184.
[41] G. Cacciapaglia, A. Deandrea, and M. Hashimoto, Phys. Rev. Lett. **115**, 171802 (2015), 1507.03098.
[42] V. Sanz (2015), 1507.03553.
[43] C.-H. Chen and T. Nomura, Phys. Lett. **B749**, 464 (2015), 1507.04431.
[44] Y. Omura, K. Tobe, and K. Tsumura, Phys. Rev. **D92**, 055015 (2015), 1507.05028.
[45] W. Chao (2015), 1507.05310.
[46] S. Fichet and G. von Gersdorff (2015), 1508.04814.
[47] C.-H. Chen and T. Nomura (2015), 1509.02039.
[48] D. Aristizabal Sierra, J. Herrero-Garcia, D. Restrepo, and A. Vicente (2015), 1510.03437.
[49] S.-S. Xue (2015), 1506.05994.
[50] C. Petersson and R. Torre (2015), 1508.05632.
[51] R. Barbier et al., Phys. Rept. **420**, 1 (2005), hep-ph/0406039.
[52] J. P. Miller, E. d. Rafael, B. L. Roberts, and D. Stockinger, Ann. Rev. Nucl. Part. Sci. **62**, 237 (2012).
[53] R. N. Mohapatra, Phys. Rev. **D34**, 3457 (1986).
[54] M. Hirsch, H. V. Klapdor-Kleingrothaus, and S. G. Kovalenko, Phys. Rev. **D53**, 1329 (1996), hep-ph/9502385.
[55] L. E. Ibanez and G. G. Ross, Phys. Lett. **B260**, 291 (1991).
[56] H. Nishino et al. (Super-Kamiokande), Phys. Rev. Lett. **102**, 141801 (2009), 0903.0676.
[57] G. Abbiendi et al. (OPAL), Eur. Phys. J. **C33**, 149 (2004), hep-ex/0310054.
[58] R. Franceschini, Adv. High Energy Phys. **2015**, 581038 (2015).
[59] G. W. Bennett et al. (Muon g-2), Phys. Rev. **D73**, 072003 (2006), hep-ex/0602035.
[60] A. Czarnecki and W. J. Marciano, Phys. Rev. **D64**, 013014 (2001), hep-ph/0102122.
[61] P. Athron, M. Bach, H. G. Fargnoli, C. Gnendiger, R. Greifenhagen, J.-h. Park, S. Paehr, D. Stockinger, H. Stockinger-Kim, and A. Voigt (2015), 1510.08071.
[62] S. Marchetti, S. Mertens, U. Nierste, and D. Stockinger, Phys. Rev. **D79**, 013010 (2009), 0808.1530.
[63] G.-C. Cho and K. Hagiwara, Nucl. Phys. **B574**, 623 (2000), hep-ph/9912260.
[64] G. Abbiendi et al. (OPAL), Eur. Phys. J. **C35**, 1 (2004), hep-ex/0401026.
[65] G. Aad et al. (ATLAS), Phys. Rev. **D91**, 052007 (2015), 1407.1376.
[66] V. Khachatryan et al. (CMS), Phys. Rev. **D91**, 052009 (2015), 1501.04198.
[67] V. Khachatryan et al. (CMS) (2015), 1512.01224.
[68] G. Aad et al. (ATLAS) (2015), 1512.01530.
[69] H. K. Dreiner and T. Stefaniak, Phys. Rev. **D86**, 055010 (2012), 1201.5014.
[70] M. E. Peskin and T. Takeuchi, Phys. Rev. Lett. **65**, 964 (1990), URL `http://link.aps.org/doi/10.1103/PhysRevLett.65.964`.
[71] M. Bahr et al., Eur. Phys. J. **C58**, 639 (2008), 0803.0883.
[72] J. Bellm et al. (2015), 1512.01178.
[73] F. Dias, S. Gadatsch, M. Gouzevich, C. Leonidopoulos, S. Novaes, A. Oliveira, M. Pierini, and T. Tomei (2015), 1512.03371.
[74] B. C. Allanach, A. Dedes, and H. K. Dreiner, Phys. Rev. **D69**, 115002 (2004), [Erratum: Phys. Rev.D72,079902(2005)], hep-ph/0309196.
[75] J. R. Ellis, J. Giedt, O. Lebedev, K. Olive, and M. Srednicki, Phys. Rev. **D78**, 075006 (2008), 0806.3648.
[76] M. Sher, Phys. Rept. **179**, 273 (1989).
[77] J. E. Camargo-Molina, B. O'Leary, W. Porod, and F. Staub, Eur. Phys. J. **C73**, 2588 (2013), 1307.1477.
[78] Y. Okada, M. Yamaguchi, and T. Yanagida, Phys. Lett. **B262**, 54 (1991).
[79] G.-C. Cho, S. Kaneko, and A. Omote, Phys. Lett. **B652**, 325 (2007), hep-ph/0611240.
[80] S. A. Abel and C. A. Savoy, Nucl. Phys. **B532**, 3 (1998), hep-ph/9803218.
[81] A. Dedes, S. Rimmer, J. Rosiek, and M. Schmidt-Sommerfeld, Phys. Lett. **B627**, 161 (2005), hep-

ph/0506209.
[82] K. Desch, S. Fleischmann, P. Wienemann, H. K. Dreiner, and S. Grab, Phys. Rev. **D83**, 015013 (2011), 1008.1580.
[83] A. Alloul, N. D. Christensen, C. Degrande, C. Duhr, and B. Fuks, Comput. Phys. Commun. **185**, 2250 (2014), 1310.1921.
[84] J. Alwall, R. Frederix, S. Frixione, V. Hirschi, F. Maltoni, O. Mattelaer, H. S. Shao, T. Stelzer, P. Torrielli, and M. Zaro, JHEP **07**, 079 (2014), 1405.0301.
[85] R. D. Ball et al., Nucl. Phys. **B867**, 244 (2013), 1207.1303.
[86] M. Agostini et al. (GERDA), Phys. Rev. Lett. **111**, 122503 (2013), 1307.4720.
[87] A. Faessler, S. Kovalenko, F. Simkovic, and J. Schwieger, Phys. Rev. Lett. **78**, 183 (1997), hep-ph/9612357.
[88] B. C. Allanach, C. H. Kom, and H. Pas, JHEP **10**, 026 (2009), 0903.0347.
[89] V. Khachatryan et al. (CMS), JHEP **08**, 174 (2014), 1405.3447.
[90] Tech. Rep. ATLAS-CONF-2015-045, CERN, Geneva (2015).
[91] Tech. Rep. CMS-PAS-EXO-14-010, CERN, Geneva (2015).
[92] G. Aad et al. (ATLAS), Eur. Phys. J. **C75**, 263 (2015), 1503.08089.
[93] V. Khachatryan et al. (CMS) (2015), 1506.01443.
[94] S. P. Liew and S. Shirai (2015), 1507.08273.
[95] V. Khachatryan et al. (CMS), Eur. Phys. J. **C74**, 3149 (2014), 1407.3683.
[96] Tech. Rep. CMS-PAS-EXO-12-041, CERN, Geneva (2014).
[97] B. Allanach, S. Biswas, S. Mondal, and M. Mitra, Phys. Rev. **D91**, 011702 (2015), 1408.5439.
[98] B. C. Allanach, S. Biswas, S. Mondal, and M. Mitra, Phys. Rev. **D91**, 015011 (2015), 1410.5947.
[99] G. Aad et al. (ATLAS) (2015), 1512.05099.